Generalized Finite Difference Method for Solving Viscoelastic Problems

Jian Li and Tao Zhang

Abstract In this paper, the generalized finite difference method (GFDM) combined with the implicit Euler method is developed to solve the viscoelastic problem. The mathematical description of the viscoelastic problem is a time-dependent boundary value problem, governed by a second-order partial differential equation and non-linear boundary conditions. To solve the time-dependent differential governing equation and boundary conditions of viscoelasticity, the implicit Euler method and GFDM are employed for the temporal discretization and the spatial discretization respectively. GFDM is a newly developed meshless method, which avoids time-consuming mesh generation and numerical integration. The basic idea of the GFDM originates from the moving least squares method to transform the spatial derivatives at each node into linear summation of nearby node function values with different weighting coefficients. Two numerical examples are presented to illustrate the accuracy, stability and efficiency of GFDM, including the creep and stress relaxation of viscoelastic materials with single connected domains and double connected domains.

Keywords Generalized finite difference method · Viscoelastic problem

1 Introduction

Viscoelastic problems are very common in engineering, such as the creep of clay or rock, which can be regarded as a class of time-dependent boundary value problems. For the simple viscoelastic problem, the analytic solutions can be obtained. But for the complex engineering problems, numerical methods are inevitably required.

Finite element method (FEM) [1, 2] and boundary element method (BEM) [3, 4] were initially used to solve the viscoelastic problem, while the element would be distorted in the process of calculation and this reduced the accuracy and led to the

J. Li · T. Zhang (✉)
Beijing Institute of Technology, Beijing 100000, China
e-mail: taozhang@bit.edu.cn

S. N. Atluri and I. Vušanović (eds.), *Computational and Experimental Simulations in Engineering*, Mechanisms and Machine Science 98,
https://doi.org/10.1007/978-3-030-67090-0_35

failure of calculation. The meshless method which was based only on node information could partially or completely avoid element constraints. So it was widely used to solve the viscoelastic problems [5–8].

The GFDM, which preserves the accuracy and simplicity of the traditional finite difference method and avoids the time-consuming meshing generation and numerical integration, is a developable meshless method proposed by Benito et al. [9] in 2001. GFDM is based on the moving-least squares method to transform the partial derivative at each node into the linear summation of the nearby node function values with different weight function. Each internal node and boundary node is forced to respectively satisfy the governing equation and boundary conditions. Then the partial differential equations will be transformed into linear algebraic equations that can be written as sparse matrix and solved easily. The GFDM preserves the physical conservation of the original equation (including the conservation of mass, momentum, energy, etc.) and other important characteristics in the subdomain. It is an important discrete method for solving the partial differential equations. Moreover, GFDM can be used to accurately and efficiently solve various problems, such as dynamic propagation of crack, impact and collision, large deformation and complex high-dimensional geometric problems and so on.

In this paper, the GFDM is extended for the first time to solve the viscoelastic problem. The outline of this paper is as follows: In Sect. 2, The temporal and special discretization of governing equation and boundary condition by implicit Euler method and GFDM is introduced. In Sect. 3, Two examples are presented to illustrate the stability, accuracy and efficiency of the proposed method. In Sect. 4, a brief summary of this paper is provided.

2 The Generalized Finite Difference Method for Viscoelastic Problem

2.1 Basic Equation of Viscoelastic Problem

The three-parameter viscoelastic model is used to descript the viscoelasticity behavior. The constitutive equations of this model are

$$\varepsilon(t) = \frac{1}{E_2} G\sigma(t), \quad t = 0 \tag{1}$$

$$q_0\varepsilon(t) + q_1\frac{d\varepsilon(t)}{dt} = G\left(\sigma(t) + p_1\frac{d\sigma(t)}{dt}\right), \quad t > 0 \tag{2}$$

where

$$p_1 = \frac{\eta_1}{E_1 + E_2}, q_0 = \frac{E_1 E_2}{E_1 + E_2}, q_1 = \frac{E_2 \eta_1}{E_1 + E_2}, \tag{3}$$

$$G = \begin{pmatrix} G_{11} & G_{12} & 0 \\ G_{12} & G_{22} & 0 \\ 0 & 0 & G_{33} \end{pmatrix}. \tag{4}$$

For the plane stress problem,

$$G_{11} = G_{22} = 1, G_{33} = 2(1+v), G_{12} = -v, \tag{5}$$

where v is Poisson's ratio.
The strain–displacement relationship can be written as

$$\varepsilon_{ij} = \left(u_{i,j} + u_{j,i}\right)/2. \tag{6}$$

The equilibrium equation of viscoelasticity is

$$\sigma_{ij,j} + b_i = 0, \tag{7}$$

and the boundary conditions are specified by:

$$u = \tilde{u} \quad \text{on } \Gamma_u, \tag{8}$$

$$\mathrm{p} = \tilde{\mathrm{p}} \quad \text{on } \Gamma_t, \tag{9}$$

where σ and ε are the stress and strain respectively; b is the body force; u is the displacement; p is the traction; $\tilde{u}$ and $\tilde{p}$ are the prescribed values of u and p on the boundary.

2.2 Generalized Finite Difference Method for Viscoelastic Problem

After the time term of the governing equation and boundary conditions are discretized by implicit Euler method, The GFDM is used to discretize the space terms of governing equations and boundary conditions. At the beginning, the interesting domain is discretized into regularly or randomly distributed boundary nodes and internal nodes. A node xi is selected as the center node, the m nodes x_j (j = 1, 2, …, m) around the x_i will be searched according to the principle of nearest distance, the node x_i and m nearest nodes are used to form a star, which is shown in Fig. 1. Assume the u_i is the displacement at point x_i and u_j is the displacement at point x_j. Using the Taylor series expansion, we can expand the u_j as:

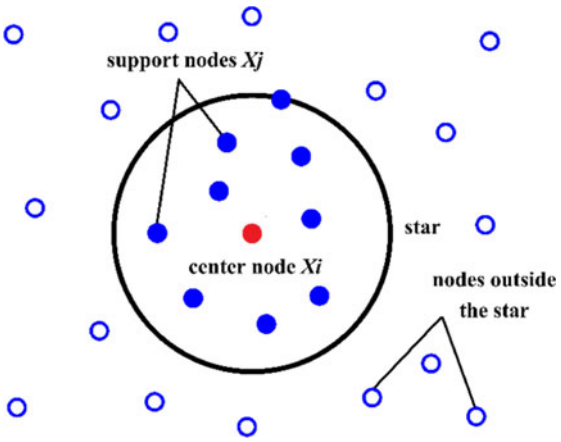

Fig. 1 The circular shape of the star

$$u_j = u_i + h_{j,i}\frac{\partial u_i}{\partial x} + k_{j,i}\frac{\partial u_i}{\partial y} + \frac{1}{2}h_{j,i}^2\frac{\partial^2 u_i}{\partial x^2} + \frac{1}{2}k_{j,i}^2\frac{\partial^2 u_i}{\partial y^2} + h_{j,i}k_{j,i}\frac{\partial^2 u_i}{\partial x \partial y} + \cdots\cdots, \quad (10)$$

where $h_{j,i} = x_j - x_i, k_{j,i} = y_j - y_i$ are the distances between x_i and x_j in x and y directions respectively. The accurate of u_j will be higher if the order of Taylor series increase. Here, the Eq. (10) is truncated after the second-order derivatives. A residual function is defined as:

$$B(u) = \sum_{j=1}^{m}\left[\left(\begin{array}{l} u_i - u_j + h_{j,i}\frac{\partial u_i}{\partial x} + k_{j,i}\frac{\partial u_i}{\partial y} + \frac{1}{2}h_{j,i}^2\frac{\partial^2 u_i}{\partial x^2} \\ + \frac{1}{2}k_{j,i}^2\frac{\partial^2 u_i}{\partial y^2} + h_{j,i}k_{j,i}\frac{\partial^2 u_i}{\partial x \partial y} \end{array}\right) w\left(h_{j,i}, k_{j,i}\right)\right]^2, \quad (11)$$

where $w\left(h_{j,i}, k_{j,i}\right)$ is the weighting function at x_i. There are many choices for $w\left(h_{j,i}, k_{j,i}\right)$, such as potential function, exponential function, cubic spline, quartic spline, etc. The quartic spline is chosen as the weighting function in this study:

$$w(d_{ij}) = \begin{cases} 1 - 6\left(\frac{d_{ij}}{dm_i}\right)^2 + 8\left(\frac{d_{ij}}{dm_i}\right)^3 - 3\left(\frac{d_{ij}}{dm_i}\right)^4, d_{ij} \le dm_i \\ 0,\ d_{ij} > dm_i \end{cases}, \quad (12)$$

where d_{ij} denotes the distance between nodes x_i and x_j, dm_i denotes the distance between the farthest node and the center node in the star.

By minimizing the above function $B(u)$ with respect to $D_u = \left\{\frac{\partial u_i}{\partial x}, \frac{\partial u_i}{\partial y}, \frac{\partial^2 u_i}{\partial x^2}, \frac{\partial^2 u_i}{\partial y^2}, \frac{\partial^2 u_i}{\partial x \partial y}\right\}^T$, a linear equation system is obtained by:

$$AD_u = b, \quad (13)$$

The vector b in Eq. (13) can be reformulated as the following form

$$b = BQ, \tag{14}$$

where $Q = \begin{bmatrix} u_i & u_1^i & u_2^i & \cdots & u_m^i \end{bmatrix}^T$ are the displacement of the total nodes inside the star. Therefore, D_u can be written as:

$$D_u = \begin{bmatrix} \frac{\partial u_i}{\partial x} \\ \frac{\partial u_i}{\partial y} \\ \frac{\partial^2 u_i}{\partial x^2} \\ \frac{\partial^2 u_i}{\partial y^2} \\ \frac{\partial^2 u_i}{\partial x \partial y} \end{bmatrix} = A^{-1}b = A^{-1}BQ = DQ = D \begin{bmatrix} u_i \\ u_1^i \\ u_2^i \\ \cdots \\ u_m^i \end{bmatrix}. \tag{15}$$

From the Eq. (15), we can obtain the partial derivatives of u_i at x_i by a linear combination of u_j at its supporting nodes x_j. The partial derivatives can be written as follows:

$$\left.\frac{\partial u}{\partial x}\right|_i = wx_0^i u_i + \sum_{j=1}^{m} wx_j^i u_j^i, \tag{16}$$

$$\left.\frac{\partial u}{\partial y}\right|_i = wy_0^i u_i + \sum_{j=1}^{m} wy_j^i u_j^i, \tag{17}$$

$$\left.\frac{\partial^2 u}{\partial x^2}\right|_i = wxx_0^i u_i + \sum_{j=1}^{m} wxx_j^i u_j^i, \tag{18}$$

$$\left.\frac{\partial^2 u}{\partial y^2}\right|_i = wyy_0^i u_i + \sum_{j=1}^{m} wyy_j^i u_j^i, \tag{19}$$

$$\left.\frac{\partial^2 u}{\partial x \partial y}\right|_i = wxy_0^i u_i + \sum_{j=1}^{m} wxy_j^i u_j^i, \tag{20}$$

where $\left\{wx_j^i\right\}_{j=0}^m, \left\{wy_j^i\right\}_{j=0}^m, \left\{wxx_j^i\right\}_{j=0}^m, \left\{wyy_j^i\right\}_{j=0}^m, \left\{wxy_j^i\right\}_{j=0}^m$ are weight coefficients of the center node x_i.

The implementing procedure at each node inside the computational domain can be carried out as described above. And the derivatives at each node will be replaced with the linear combination of the approximate nodal values. Each interior node is forced to satisfy the governing equation and each boundary node is forced to satisfy the boundary condition. The partial differential equations will be transformed into linear (or nonlinear) algebraic equations.

3 Numerical Examples

3.1 Example 1: Creep Analysis of a Rectangular Plate

The first example is a rectangular viscoelastic plate subjected to a uniform traction loading $P = 1\,\mathrm{N/m^2}$ at the right end $x = L$. The left and lower ends are fixed in the x-direction and y-direction respectively and the other boundary is free, as shown in Fig. 2. The material parameters are $E_1 = 1000\,\mathrm{N/m^2}$,$E_2 = 2000\,\mathrm{N/m^2}$, $\eta = 1000\,\mathrm{N/m^2}$, and $v = 0.3$. The length of the plate is $L = 2\,\mathrm{m}$ and the width is $w = 1\,\mathrm{m}$. The analytical solutions of displacements are given as follows:

$$u_x = Px\left(\frac{1}{E_2} + \frac{1}{E_1}\left(1 - e^{-\frac{\eta_1}{E_1}t}\right)\right), \tag{21}$$

$$u_y = -vPy\left(\frac{1}{E_2} + \frac{1}{E_1}\left(1 - e^{-\frac{\eta_1}{E_1}t}\right)\right). \tag{22}$$

In this example, 60 boundary nodes and 171 internal nodes are used, see Fig. 3. In Fig. 4 and Fig. 5, The numerical results for the variation of displacement from t = 0 s to t = 10 s at nodes A (2, 0.5) and B (1, 1) obtained by the present method are compared with analytical results. We can observe a very good agreement of both results.

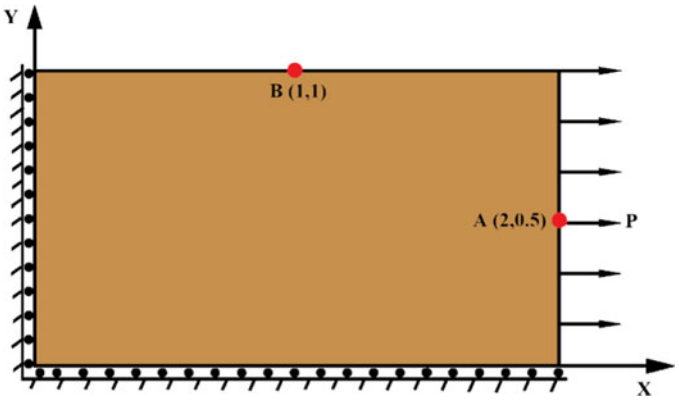

Fig. 2 The geometry for example 1

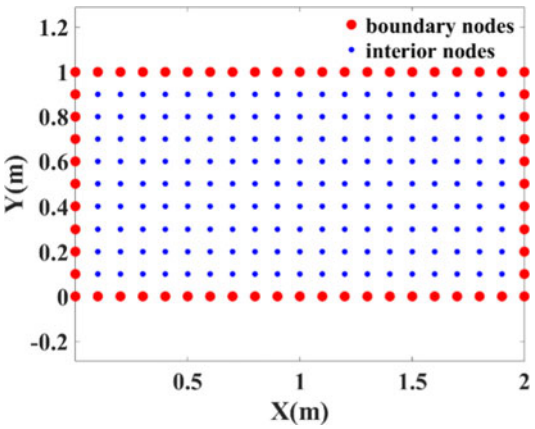

Fig. 3 The nodes distribution for example 1

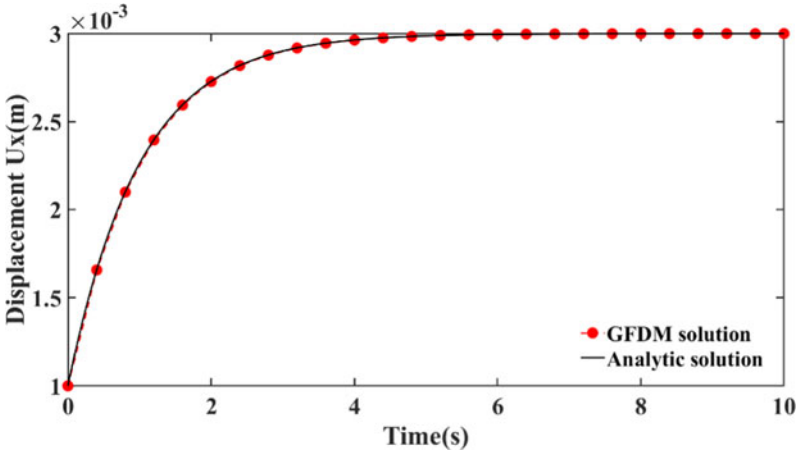

Fig. 4 The variation of displacement at point A (2, 0.5) from t = 0 s to t = 10 s

3.2 *Example 2: Relaxation Analysis of a Square Plate with a Circular Hole*

The second example is a square plate with a circular hole at the center subjected to a uniform displacement $u_0 = 5 \times 10^{-4}$ m, as shown in Fig. 6. The side length is $W = 20$ m, and the radius of circular hole is $R = 5$ m. The material parameters are given as:$E_1 = 1000\,\text{N/m}^2, E_2 = 2000\,\text{N/m}^2, \eta_1 = 1000\,\text{N/m}^2$, and $\nu = 0.3$.

Due to the symmetry of the model, only one quarter of the plate is considered as shown in Fig. 7. The total number of nodes is 813 as shown in Fig. 8. As there is no analytical solution, a convergent ABAQUS viscoelastic solution with 98,102 element nodes is used as reference. In the ABAQUS model, only quadrilateral element is used.

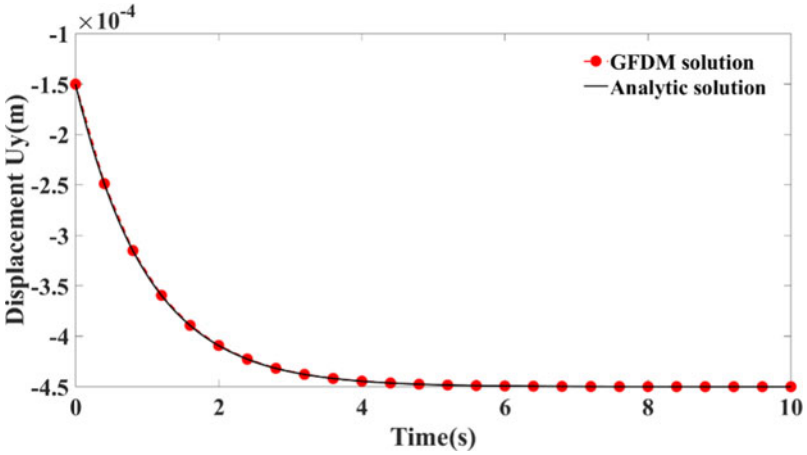

Fig. 5 The variation of displacement at point B (1, 1) from t = 0 s to t = 10 s

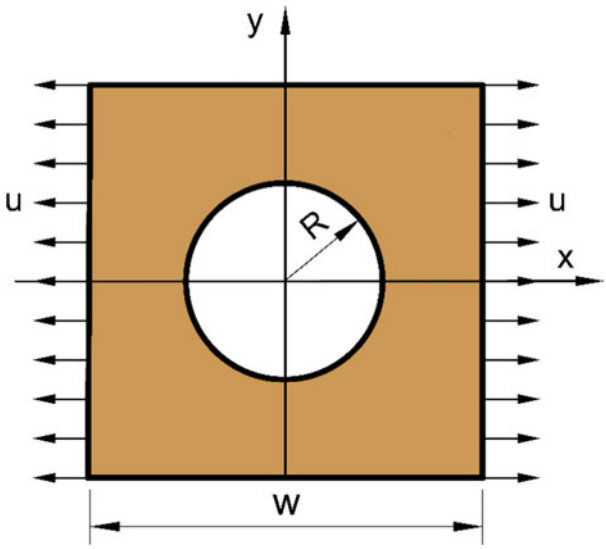

Fig. 6 Geometry model for example 2

Since there is stress concentration in the circular hole of the plate, it is difficult to obtain the accurate results of stress in the circular hole. The fourth-order Taylor series is used to obtain the accurate numerical results in the numerical procedures of

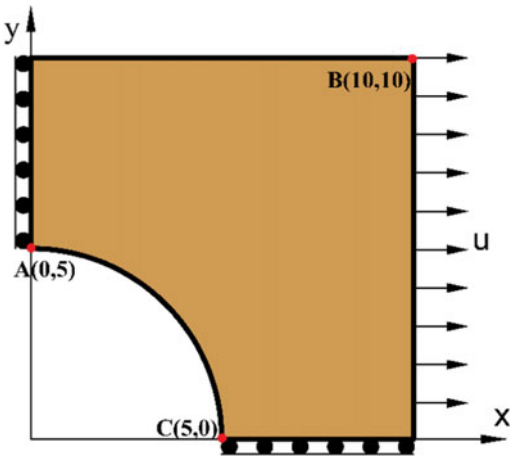

Fig. 7 Simplified model for example 2

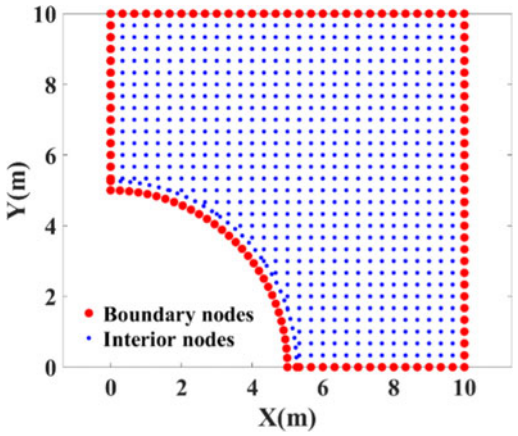

Fig. 8 The nodes distribution for example 2

GFDM. In Fig. 9, Fig. 10 and Fig. 11, the variation of stress from t = 0 s to t = 2 s at nodes A (0, 5), B (10, 10) and C (5, 0) obtained by the present method are compared with the reference results. We can observe that the results obtained using GFDM are in good agreement with the ABAQUS solution.

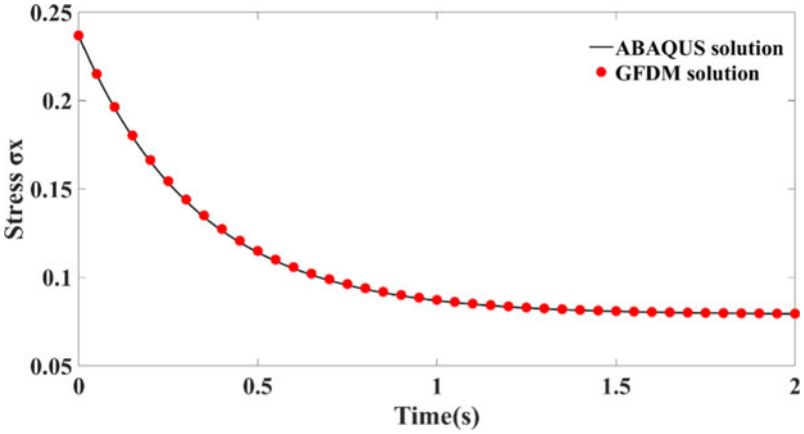

Fig. 9 The variation of stress at points A (0, 5) from t = 0 s to t = 2 s

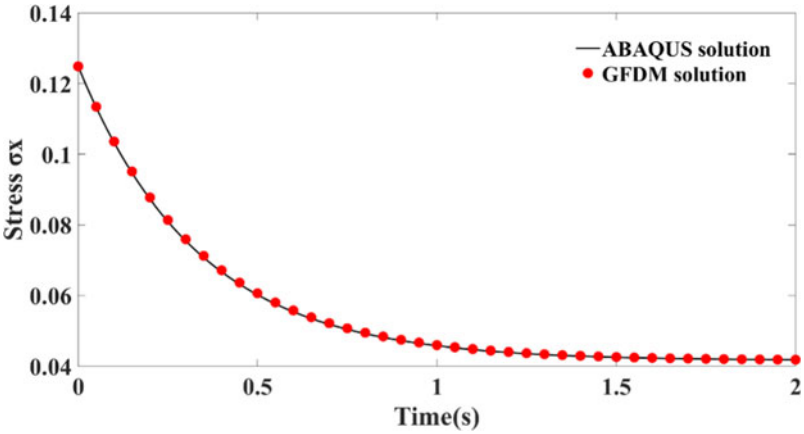

Fig. 10 The variation of stress at points B (10, 10) from t = 0 s to t = 2 s

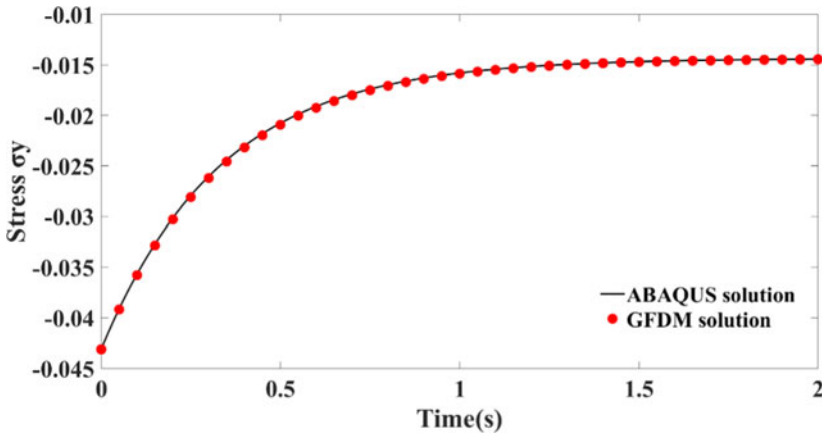

Fig. 11 The variation of stress at points C (5, 0) from t = 0 s to t = 2 s

4 Conclusions

In this paper, the GFDM and the implicit Euler method are adopted to discretized spatial and temporal domain of viscoelastic problem respectively. As the viscoelastic material are often accompanied by continuous shape deformation, the meshless method is a better choice. GFDM is a newly-developed domain-type meshless method, which really avoids time-consuming mesh generation and numerical integration. So it has a simple form and high calculation efficiency. Two examples are proposed to prove the simplicity and efficiency of the proposed method for viscoelastic problems.

References

1. Chen, W.H., Lin, T.C.: Dynamic analysis of viscoelastic structures using incremental finite element method. Eng. Struct. **4**(4), 271–276 (1982)
2. Mesquita, A.D., Coda, H.B.: Alternative Kelvin viscoelastic procedure for finite elements. Appl. Math. Model. **26**(4), 501–516 (2002)
3. Yang, H., Guo, X.: Perturbation boundary–finite element combined method for solving the linear creep problem. Int. J. Solids Struct. **37**(15), 2167–2183 (2000)
4. Mesquita, A.D., Coda, H.B., Venturini, W.S.: Alternative time marching process for BEM and FEM viscoelastic analysis. Int. J. Numer. Method Eng. **51**, 1157–1173 (2001)
5. Haitian, Y., Yan, L.: A combined approach of EFGM and precise algorithm in time domain solving viscoelasticity problems. Int. J. Solids Struct. **40**(3), 701–714 (2003)

6. Sladek, J., Sladek, V., Zhang, C., et al.: Meshless local Petrov-Galerkin method for continuously nonhomogeneous linear viscoelastic solids. Comput. Mech. **37**(3), 279–289 (2006)
7. Miao-Juan, P., Qian, L.: Improved complex variable element-free Galerkin method for viscoelasticity problems. Acta Physica Sinica **63**(18), 180203–180203 (2014)
8. Peng, M.J., Li, R.X., Cheng, Y.M.: Analyzing three-dimensional viscoelasticity problems via the improved element-free Galerkin (IEFG) method. Eng. Anal. Bound. Elem. **40**, 104–113 (2014)
9. Benito, J.J., Urena, F., Gavete, L.: Influence of several factors in the generalized finite difference method. Appl. Math. Model. **25**(12), 1039–1053 (2001)